Coulomb excitation of unstable nuclei at intermediate energies

C.A. Bertulani[1], G. Cardella[2], M. De Napoli[2,3], G. Raciti[2,3], and E. Rapisarda[2,3]

[1] *Department of Physics and Astronomy,*

University of Tennessee, Knoxville, Tennessee 37996, USA

[2] *Istituto Nazionale di Fisica Nucleare, Sezione di Catania,*

via Santa Sofia 64, I-95123, Catania, Italy

[3] *Dipartimento di Fisica e Astronomia, Universitá Catania,*

via Santa Sofia 64, I-95123, Catania, Italy

arXiv:0704.0060v1 [nucl-th] 31 Mar 2007

Abstract

We investigate the Coulomb excitation of low-lying states of unstable nuclei in intermediate energy collisions ($E_{lab} \sim 10-500$ MeV/nucleon). It is shown that the cross sections for the $E1$ and $E2$ transitions are larger at lower energies, much less than 10 MeV/nucleon. Retardation effects and Coulomb distortion are found to be both relevant for energies as low as 10 MeV/nucleon and as high as 500 MeV/nucleon. Implications for studies at radioactive beam facilities are discussed.

PACS numbers: 25.60.-t, 25.70.-z, 25.70.De

Keywords: Coulomb excitation, cross sections, unstable nuclei.

Unstable nuclei are often studied with reactions induced by secondary radioactive beams. Examples of these reactions are elastic scattering, fragmentation and Coulomb excitation by heavy targets. Coulomb excitation is specially useful since the interaction mechanism is very well known [1]. It is the result of electromagnetic interactions of a projectile (Z_P,A_P) with a target (Z_T,A_T). One of the participating nuclei is excited as it passes through the electromagnetic field of the other. Here we will only consider the excitation of the projectile as is of interest in studies carried out in heavy ion facilities around the world, e.g. LNS/Catania, NSCL/MSU, GSI, GANIL, RIKEN, etc. In Coulomb excitation a virtual photon with energy E is absorbed by the projectile. Because in pure Coulomb excitation the participating nuclei stay outside the range of the nuclear strong force, the excitation cross section can be expressed in terms of the same multipole matrix elements that characterize excited-state gamma-ray decay, or the reduced transition probabilities, $B(\pi\lambda; J_i \rightarrow J_f)$. Hence, Coulomb excitation amplitudes are strongly coupled with valuable nuclear structure information. Therefore, this mechanism has been used for many years to study the electromagnetic properties of low-lying nuclear states [1].

Coulomb excitation cross sections are large if the adiabacity parameter satisfies the condition

$$\xi = \omega_{fi}\frac{a_0}{v} < 1 \ , \tag{1}$$

where a_0 is half the distance of closest approach in a head-on collision for a projectile velocity v, and $E_x = \hbar\omega_{fi}$ is the excitation energy. This adiabatic cut-off limits the possible excitation energies below 1-2 MeV in sub-barrier collisions. A possible way to overcome this limitation, and to excite high-lying states, is to use higher projectile energies. In this case, the closest approach distance, at which the nuclei still interact only electromagnetically, is of order of the sum of the nuclear radii, $R = R_P + R_T$, where P refers to the projectile and T to the target. For very high energies one has also to take into account the Lorentz contraction of the interaction time by means of the Lorentz factor $\gamma = (1 - v^2/c^2)^{-1/2}$, with c being the speed of light. For such collisions the adiabacity condition, Eq. (1), becomes

$$\xi(R) = \frac{\omega_{fi}R}{\gamma v} < 1 \ . \tag{2}$$

From this relation one obtains that for bombarding energies around and above 100 MeV/nucleon, states with energy up to 10-20 MeV can be readily excited [3].

An appropriate description of Coulomb excitation at intermediate energies (E_{lab} =

$10 - 500$ MeV/nucleon) has been described in ref. [2]. In this energy region neither the non-relativistic Coulomb excitation formalism described in ref. [1], nor the relativistic one formulated in refs. [3, 4] are appropriate. This is discussed in details in ref. [2] where it is shown that the correct values of the Coulomb excitation cross sections differ by up to 30-40% when compared to the non-relativistic and relativistic treatments used to calculate experimental observables (cross sections, gamma-ray angular distributions, etc.).

We follow the formalism of ref. [2] to calculate cross sections for Coulomb excitation from energies varying from 10 to 500 MeV/nucleon. These are the energies where most radioactive beam facilities are or will be operating around the world. The calculated cross sections will be of useful guide for future experiments. We also compare the accurate calculations with those obtained by using simple analytical formulas and test the regime of their validity.

The cross sections for the transition $J_i \rightarrow J_f$ in the projectile are calculated using the equation [2]

$$\frac{d\sigma_{i\rightarrow f}}{d\Omega} = \frac{4\pi^2 Z_T^2 e^2}{\hbar^2}\, a^2\epsilon^4 \sum_{\pi\lambda\mu} \frac{B(\pi\lambda, J_i \rightarrow J_f)}{(2\lambda+1)^3} \mid S(\pi\lambda,\mu) \mid^2 , \tag{3}$$

where $\pi = E$ or M stands for the electric or magnetic multipolarity, and

$$B(\pi\lambda, J_i \longrightarrow J_f) = \frac{1}{2J_i+1} \; |\langle J_f \,\|\mathcal{M}(\pi\lambda)\|\, J_i\rangle|^2 \tag{4}$$

are the reduced transition probabilities. In these equations, $\epsilon = 1/\sin(\Theta/2)$, with Θ being the deflection angle, $a_0 = Z_P Z_T e^2/m_0 v^2$ and $a = a_0/\gamma$. The complex functions $S(\pi\lambda,\mu)$ are integrals along Coulomb trajectories corrected for retardation. Their calculation and how they relate to the non-relativistic and relativistic theories are described in details in ref. [2]. Here we will introduce another comparison tool for the total cross section, which is obtained by integration of eq. 3 over scattering angles. The code COULINT [2] was used to calculate the orbital integrals $S(\pi\lambda,\mu)$ and the cross sections of eq. 3 (for more details, see ref. [2]).

Using the theory described in ref. [4], it is easy to show that approximate values of the cross sections for E1, E2, and M1 transitions can be obtained by means of the relations

$$\begin{aligned}
\sigma_{E1}^{(app)} &= \frac{32\pi^2}{9}\frac{Z_T^2\alpha}{\hbar c} B\,(E1)\left(\frac{c}{v}\right)^2 \left[\xi K_0 K_1 - \frac{v^2\xi^2}{2c^2}\left(K_1^2 - K_0^2\right)\right] \\
\sigma_{E2}^{(app)} &= \frac{8\pi^2}{75}\frac{Z_T^2\alpha}{(\hbar c)^3} E_x^3 B\,(E2)\left(\frac{c}{v}\right)^4 \left[\frac{2}{\gamma^2}K_1^2 + \xi\left(1+\frac{1}{\gamma^2}\right)^2 K_0 K_1 - \frac{v^4\xi^2}{2c^4}\left(K_1^2 - K_0^2\right)\right] \\
\sigma_{M1}^{(app)} &= \frac{32\pi^2}{9}\frac{Z_T^2\alpha}{\hbar c} B\,(M1)\left[\xi K_0 K_1 - \frac{\xi^2}{2}\left(K_1^2 - K_0^2\right)\right],
\end{aligned} \tag{5}$$

where K_n are the modified Bessel functions of the second order, as a function of ξ given by eq. 2, with R corrected for recoil by the modification $R \to R + \pi a/2$ [3].

Here we will only consider the excitation of the lowest lying states in light and medium heavy nuclei. For nuclear masses $A < 20$, the TUNL nuclear data evaluation web site was of great help [5]. The electromagnetic transition rates at the TUNL database are given in Weisskopf units and are transformed to the appropriate $B(\pi\lambda, I_i \to I_f)$-values by means of the standard Weisskopf relations $B(E1; J_i \to J_{gs}) = 0.06446 A^{2/3}$ e^{2}fm^2, $B(E2; J_i \to J_{gs}) = 0.05940 A^{4/3}$ e^{2}fm^4, and $B(M1; J_i \to J_{gs}) = 1.79\,(e\hbar/2m_n c)^2$. For comparison, a few medium mass nuclei, as well as a few stable nuclei, were included in the calculation. Other data were taken from refs. [6, 7, 8, 9].

Some cases of nuclei far from the stability line are very interesting and deserve further study, possibly using the method of Coulomb excitation. For example, it is well known that nuclei with open shells tend to have $B(E2)$ values greater than 10 W.u., whereas nuclei with shell closure of neutrons or protons tend to have distinctly smaller $B(E2)$ values. Typical examples of the latter category are the doubly magic nuclei, ^{16}O and ^{48}Ca, which $B(E2)$ values are 3.17 and 1.58 W.u., respectively. According to an empirical formula adjusted to a global fit of the known transition rates, the values of first excited 2^+ level, E_{2^+}, and $B(E2; 0^+ \to 2^+)$ are related by [10]

$$B(E2; 0^+ \to 2^+) = 26 \frac{Z^2}{A^{2/3} E_{2^+}} \text{ e}^2\text{fm}^4. \tag{6}$$

The value of $B(E2)$ for ^{16}C based on this formula is at least one order of magnitude larger than what is observed experimentally [9]. The anomalously strong hindrance of the ^{16}C transition is not well explained theoretically. This is just an example of the power of Coulomb excitation as a tool to access the new physics inherent of poorly known rare nuclear species.

Another example is the strong $E1$ transition in ^{11}Be. ^{11}Be is an archetype of a halo nucleus and exhibits the fastest known dipole transition between bound states in nuclei. The $B(E1)$ transition strength between the ground and the only bound excited state (at 0.32 MeV) was determined from lifetime measurements by Millener et al. to be 0.116 e^{2}fm^2 [11]. However, Coulomb excitation experiments have obtained a much smaller value of the $B(E1)$ which is still a matter of investigation [12, 13, 14]. It is thus seems clear that predictions based on traditional nuclear structure and reaction theory often yields results in disagree-

ment with experimental data. In spite of that, when proper corrections are accounted for (e.g. channel-coupling, nuclear excitation, relativistic corrections), Coulomb excitation of radioactive beams is a powerful complementary tool to investigate electromagnetic properties of nuclei far from the stability line.

In Table 1 we compare our calculations with several experimentally obtained cross sections for Coulomb excitation of unstable nuclei. The units of energy are MeV, the laboratory energy is in MeV/nucleon, the B-values are in units of e^2 $fm^{2\lambda}$, and the cross sections are in millibarns. The last two columns give the calculated cross sections obtained by using eqs. 3 and 5, respectively. Except for the ^{11}Be case, for which the discrepancy between theory and experiment are known (see discussion above), the calculated cross sections are close to the experimental values. Nonetheless, the calculated cross sections tend to be smaller than the experimental ones for ^{17}Ne, ^{32}Mg, ^{38}S, ^{40}S, ^{42}S, ^{44}Ar, and ^{46}Ar projectiles. This is worrisome because the B($\pi\lambda$) values were extracted from the experimentally obtained cross sections, using equations similar to eq. 5. These experimental B-values would have to be larger by $10 - 30\%$ according to our calculations.

It is important to stress the fact that many experimental data on unstable nuclei collected up to now have been analyzed by means of theoretical tools (DWBA and coupled-channels codes) which do not include relativistic dynamics (the inclusion of relativistic kinematics is straightforward). This problem was first addressed in ref. [15], where it was shown that the analysis of experimental data at intermediate energies without a proper treatment of relativistic dynamics leads to wrong values of electromagnetic transition probabilities. We should stress that a full theoretical treatment of relativistic dynamics of strong and electromagnetic interactions in many-body systems is very difficult and still does not exist [15].

Data	Projectile	Target	E_{lab}	$\pi\lambda$	$B(\pi\lambda)$	θ_{range}	E_x	σ_{exp}	σ_{th}	σ_{app}
1 [16]	^{11}Be	Pb	43.	E1	0.115	$< 5°$	0.32 ($\frac{1}{2}^+ \to \frac{1}{2}^-$)	191 ± 26	328.	323.
2 [16]	^{11}Be	Pb	59.4	E1	0.094	$< 3.8°$	0.32 ($\frac{1}{2}^+ \to \frac{1}{2}^-$)	304 ± 43	213.	211.
3 [18]	^{11}Be	Au	57.6	E1	0.079	$< 3.8°$	0.32 ($\frac{1}{2}^+ \to \frac{1}{2}^-$)	244 ± 31	170.	168.
4 [17]	^{11}Be	Pb	64.	E1	0.099	$< 3.8°$	0.32 ($\frac{1}{2}^+ \to \frac{1}{2}^-$)	302 ± 31	217.	215.
5 [19, 20]	^{17}Ne	Au	60.	M1	0.163	$< 4.5°$	1.29 ($\frac{1}{2}^- \to \frac{3}{2}^-$)	12 ± 4	12.6	13.0
6 [6]	^{32}Mg	Pb	49.2	E2	454	$< 4°$	0.885 ($0^+ \to 2^+$)	91.7 ± 14.4	137.	128.
7 [19]	^{38}S	Au	39.2	E2	235	$< 4.1°$	1.29 ($0^+ \to 2^+$)	59 ± 7	48.	45.0
8 [19]	^{40}S	Au	39.5	E2	334	$< 4.1°$	0.91 ($0^+ \to 2^+$)	94 ± 9	75.5	70.4
9 [19]	^{42}S	Au	40.6	E2	397	$< 4.1°$	0.89 ($0^+ \to 2^+$)	128 ± 19	101.	94.3
10 [19]	^{44}Ar	Au	33.5	E2	345	$< 4.1°$	1.14 ($0^+ \to 2^+$)	81 ± 9	62.3	58.3
11 [19]	^{46}Ar	Au	35.2	E2	196	$< 4.1°$	1.55 ($0^+ \to 2^+$)	53 ± 10	40.9	38.2
12 [8]	^{46}Ar	Au	76.4	E2	212	$< 2.9°$	1.55 ($0^+ \to 2^+$)	68 ± 8	50.0	47.4

Table 1. Cross sections for Coulomb excitation of unstable nuclei. The units of energy are MeV, the laboratory energy is in MeV/nucleon, the $B(\pi\lambda)$-values are in units of $e^2 fm^{2\lambda}$, and the cross sections are in millibarns. The data for different experiments (numbered 1 to 12) were collected from the references listed in column 1. The last two columns give the calculated cross sections obtained by using eqs. 3 and 5, respectively.

In figure 1 we show a comparison between the experimental data and our calculations. We notice that the cross sections calculated with help of eq. 5 are not much different than those calculated with eq. 3. They are systematically lower, up to 10%, than the exact calculation following eq. 3. As we discuss below, this is not always the case, specially for the excitation of high-lying states. In fact, this is a good check of eq. 3, which is done in a very different way than the analytical calculations of eq. 5. But as we will see below, this agreement is not always the case, specially when one includes small impact parameters for which the sensitivity to the relativistic corrections is higher (see ref. [2]). The dashed curve in figure 1 is a guide to the eye. It helps to see that the experimental cross sections are on average larger than the calculated ones, either with eq. 3 (open circles), or with eq. 5 (open triangles).

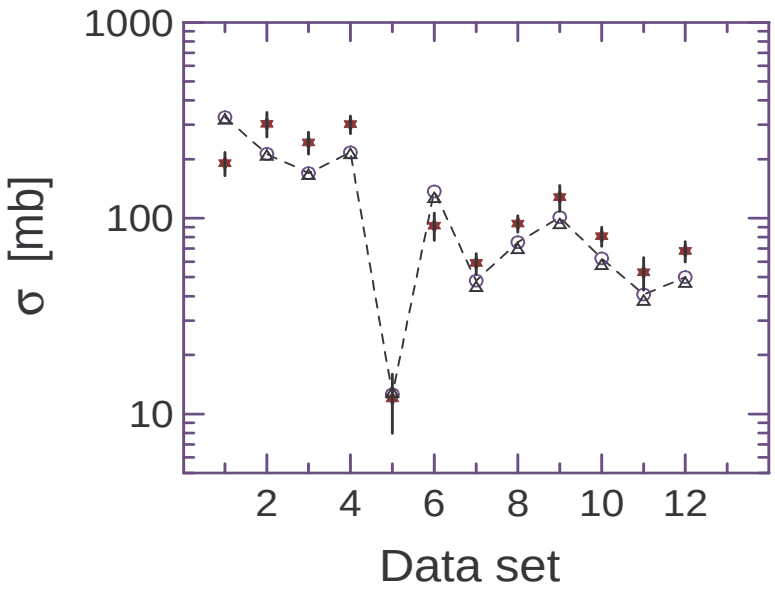

FIG. 1: Comparison between experimental Coulomb excitation cross sections (solid stars with error bars) and theoretical ones, calculated either with eq. 3 (open circles), or with eq. 5 (open triangles).

	E_x [MeV]	$J_i^\pi \to J_f^\pi$	$\pi\lambda$	$B(\pi\lambda)$ [e^2 fm$^{2\lambda}$]	10	20	30	50	100	200	500
^{11}Be	0.32	$\frac{1}{2}^- \to \frac{1}{2}^+$	E1	0.115	1128	653	473	315	187	115	69.6
^{11}B	2.21	$\frac{3}{2}^- \to \frac{1}{2}^-$	M1	2.40×10^{-2}	0.301	0.799	1.15	1.63	2.33	3.08	4.17
^{11}C	2.00	$\frac{3}{2}^- \to \frac{1}{2}^-$	M1	1.52×10^{-2}	0.196	0.551	0.793	1.12	1.57	2.07	2.76
^{12}B	0.953	$1^+ \to 2^+$	M1	4.62×10^{-3}	0.227	0.395	0.490	0.607	0.762	0.917	1.13
^{12}C	4.44	$0^+ \to 2^+$	E2	37.9	34.6	38.6	31.3	21.6	12.1	6.93	3.81
^{13}C	3.09	$\frac{1}{2}^- \to \frac{1}{2}^+$	E1	1.39×10^{-2}	8.37	11.3	11.0	9.61	7.28	5.39	3.89
^{13}N	2.37	$\frac{1}{2}^- \to \frac{1}{2}^+$	E1	3.56×10^{-2}	38.2	43.6	39.6	32.5	23.2	16.4	11.4
^{15}C	0.74	$\frac{1}{2}^+ \to \frac{5}{2}^+$	E2	2.90	8.79	4.04	2.65	1.59	0.839	0.475	0.267
^{16}C	1.77	$0^+ \to 2^+$	E2	2.12	8.81	4.41	2.92	1.76	0.920	0.517	0.285
^{16}N	0.12	$0^- \to 2^-$	E2	10.2	31.0	14.1	9.21	5.53	2.91	1.64	0.926
^{17}N	1.37	$\frac{1}{2}^- \to \frac{3}{2}^-$	M1	5.15×10^{-3}	0.153	0.304	0.397	0.516	0.680	0.848	1.09
^{17}O	0.87	$\frac{5}{2}^+ \to \frac{1}{2}^+$	E2	2.07	6.30	2.88	1.87	1.12	0.588	0.332	0.184
^{17}F	0.5	$\frac{5}{2}^+ \to \frac{1}{2}^+$	E2	21.6	68.3	29.7	19.3	11.6	6.08	3.44	1.92
^{18}O	1.98	$0^+ \to 2^+$	E2	44.8	109	60.7	40.9	24.8	11.6	7.27	3.99
^{18}F	0.94	$1^+ \to 3^+$	E2	37.9	115	52.5	34.1	20.4	10.7	6.01	3.34
^{18}Ne	1.89	$0^+ \to 2^+$	E2	248	615	342	229	138	72.0	40.1	22.1
^{19}O	0.1	$\frac{5}{2}^+ \to \frac{3}{2}^+$	M1	2.34×10^{-4}	0.0495	0.0615	0.0673	0.0737	0.0799	0.779	0.799
^{19}F	0.11	$\frac{1}{2}^+ \to \frac{1}{2}^-$	E1	5.51×10^{-4}	8.07	4.36	3.06	1.97	1.10	0.592	0.337
^{19}Ne	0.24	$\frac{1}{2}^+ \to \frac{5}{2}^+$	E2	119	361	157	102	61.6	32.5	18.5	10.5
^{20}O	1.67	$0^+ \to 2^+$	E2	28.0	72	37.4	24.9	15.1	7.86	4.41	2.43
^{20}F	0.656	$2^+ \to 3^+$	M1	3.56×10^{-3}	0.237	0.385	0.465	0.560	0.683	0.803	0.959
^{20}Ne	1.63	$0^+ \to 2^+$	E2	319	834	433	287	173	89.8	50.3	27.6
^{30}Ne	0.791	$0^+ \to 2^+$	E2	460	1167	550	361	218	115	65.0	35.2
^{32}Mg	0.885	$0^+ \to 2^+$	E2	454	1151	541	355	214	112	63.0	36.7
^{42}S	0.89	$0^+ \to 2^+$	E2	397	945	445	292	175	91.9	52	29.7
^{46}Ar	1.55	$0^+ \to 2^+$	E2	190	399	209	140	84.4	44.1	24.7	13.6
^{54}Ni	1.40	$0^+ \to 2^+$	E2	626	1319	677	447	268	139	78.1	43.1

Table 2 - Cross sections (in mb) for Coulomb excitation of projectiles incident on Pb targets at bombarding energies ranging from 10 to 500 MeV/nucleon. The energy units are MeV, the laboratory energy is in MeV/nucleon, the B($\pi\lambda$)-values are in units of e^{2}fm$^{2\lambda}$.

The cross sections for Coulomb excitation of numerous projectiles incident on Pb targets at bombarding energies ranging from 10 to 500 MeV/nucleon is shown in Table 2. These cross sections were calculated assuming that the detectors collect events from all possible Coulomb scattering events. In a real experimental situation, the angular distribution is restricted to angular windows, reducing the available cross sections. Only the lowest lying transitions have been considered, i.e. from the ground to the first excited states. One observes that some cross sections are very large, specially for ^{11}Be, ^{18}Ne, ^{30}Ne and ^{54}Ni. For these and other similar cases, the measurements are easy to perform, with a large number of events/second even with modest intensities. Cases such as ^{16}C are well within the experimental possibilities in most radioactive beam facilities.

Table 2 also shows that, except for M1 excitations, the Coulomb excitation cross sections decrease steadily as the energy increases from 10 to 500 MeV/nucleon. Based on these numbers alone, one could conclude that Coulomb excitation of low-lying states (in contrast to the case of high-lying states, e.g. giant resonances [4]) are better suited for studies at low energies. Lower energies are also less influenced by contamination due to nuclear breakup [12, 14]. Evidently this conclusion depends on the choice of the experimental setup. Identification of gamma-rays from de-excitation using Doppler shift techniques are also often more advantageous at higher energies. Except for few cases (e.g. ^{11}C), the magnetic dipole transitions are much smaller than those for $E1$ and $E2$ transitions. Even for M1 transitions the measurements are under the possibility of most new experimental facilities.

The comparison of the exact calculations, using eq. 3 (solid lines), and the approximations 5 (dashed lines) are shown in figs. 2(a-d), for ^{11}Be, ^{11}B, ^{54}Ni and ^{16}O, respectively. The ^{16}O case (as well as for ^{12}C in Table 2) was included for comparison, with a high-lying excited state. We see from figs 2a and 2b that the approximations in eq. 5 work quite well for the $M1$ multipolarity and reasonably well (within 20% at 10 MeV/nucleon and 5% at 50 MeV/nucleon) for the $E1$ cases. But they fail badly at low and intermediate energies for the $E2$ (fig. 2c). The reason is that the $E2$ Coulomb field ("tidal field") is very sensitive to the details of the collision dynamics at low energies. These conclusions can be deceiving since even for the $E1$ and $M1$ cases the approximations in eq. 5 may strongly differ from the exact calculations if the excitation energy is large (see discussion in ref. [2]). This is shown in figure 2d, where we plot the Coulomb excitation cross section of the $E_x = 13.09$

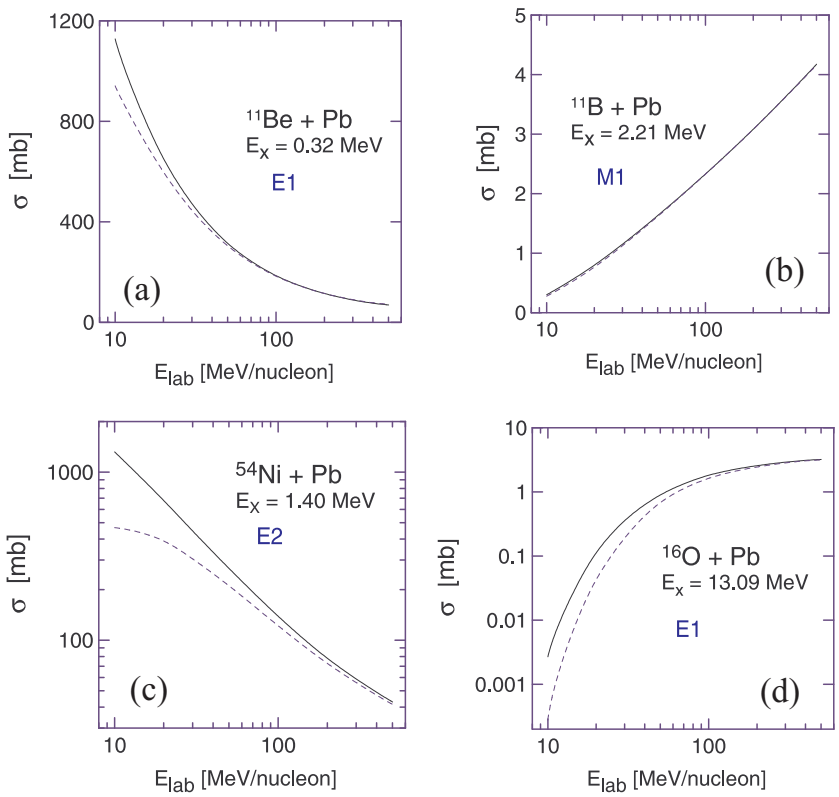

FIG. 2: Coulomb excitation cross section of the first excited state in ^{11}Be, ^{11}B and ^{54}Ni and of the 13.05 MeV sate in ^{16}O projectiles incident on Pb targets as a function of the laboratory energy.

MeV state in ^{16}O. In this case, the cross sections based on eq. 5 is a factor of 10 smaller than the exact calculation at 10 MeV/nucleon. At 100 MeV/nucleon this difference drops to 10%, which still needs to be considered with care.

In summary, in this article we have used the formalism of ref. [2] to predict the cross sections for Coulomb excitation of several light projectiles with electromagnetic transitions found in the literature, listed in the TUNL database [5], and for a few other selected cases. These estimates will be useful for planing Coulomb excitation experiments at present and future heavy ion facilities. It is evident that the inclusion of relativistic effects combined with Coulomb distortion are of the utmost relevance. The cross section inferred by using non-relativistic or pure relativistic treatments can be wrong by up to 30% even at 100 MeV/nucleon, as shown here and in ref. [2]. Finally, the use of Coulomb excitation to produce nuclei in high-lying states is an important tool to study particle emission processes. For example, the excitation of ^{18}Ne and its subsequent decay by two-proton emission is a

process of large theoretical and experimental interest. Experimental work in this direction is in progress [21].

Acknowledgments

This research was supported by the U.S. Department of Energy under contract No. DE-AC05-00OR22725 (Oak Ridge National Laboratory) with UT-Battelle, LLC., and by DE-FC02-07ER41457 with the University of Washington (UNEDF, SciDAC-2).

---

[1] K. Alder and A. Winther, Electromagnetic Excitation, North-Holland, Amsterdam, 1975.

[2] C.A. Bertulani, A.E. Stuchbery, T.J. Mertzimekis and A.D. Davies, Phys. Rev. C **68** (2003) 044609.

[3] A. Winther and K. Alder, Nucl. Phys. A **319** (1979) 518.

[4] C.A. Bertulani and G. Baur, Nucl. Phys. A **442** (1985) 739.

[5] TUNL Nuclear Data Project: http://www.tunl.duke.edu/nucldata/index.shtml

[6] T. Motobayashi et al., Phys. Lett. B **346** (1995) 9.

[7] H. Scheit et al., Phys. Rev. Lett. **77** (1996) 3967.

[8] A. Gade et al., Phys. Rev. C **68** (2003) 014302.

[9] N. Imai et al, Phys. Rev. Lett. **92** (2004) 062501.

[10] S. Raman, C.W. Nestor, Jr., and K. H. Bhatt, Phys. Rev. C **37**, 805 (1988).

[11] D. J. Millener, J. W. Olness, E. K. Warburton, and S. S. Hanna, Phys. Rev. C **28** (1983) 497.

[12] C. A. Bertulani, L. F. Canto, and M. S. Hussein, Phys. Lett. B **353** (1995) 413.

[13] M. S. Hussein, R. Lichtenthäler, F. M. Nunes, and I. J. Thompson, Phys. Lett. B **640** (2006) 91.

[14] R. Chatterjee, [Los Alamos archive: nucl-th/0703083], 2007.

[15] C.A. Bertulani, Phys. Rev. Lett. **94** (2005) 072701.

[16] R. Anne et al., Z. Phys. A **352** (1995) 397.

[17] T. Nakamura et al., Phys. Lett. B **394** (1997) 11.

[18] M. Fauerbach et al., Phys. Rev. C **56** (1997) R1.

[19] M.J. Chromik et al., Phys. Rev C **55** (1997) 1676.

[20] M.J. Chromik et al., Phys. Rev C **66** (2002) 024313.

[21] E. Rapisarda, G. Cardella, F. Amorini, L. Calabretta, M. De Napoli, P.Figuera, G. Raciti, F. Rizzo, D. Santonocito and C. Sfienti, ^{18}Ne diproton decay, *7th Int. Conf. on Radioactive Nuclear Beams*, Cortina d'Ampezzo, Italy, July 3 - 7, 2006.